

Article

Performance and Durability of the Zr-Doped CaO Sorbent under Cyclic Carbonation–Decarbonation at Different Operating Parameters

Vyacheslav V. Rodaev * and Svetlana S. Razlivalova

Institute for Nanotechnology and Nanomaterials, Derzhavin Tambov State University, Internatsionalnaya Str. 33, 392000 Tambov, Russia; razlivalova8@yandex.ru

* Correspondence: rodav1980@mail.ru; Tel.: +7-910-6522328; Fax: +7-4752-532680

Abstract: The effect of cyclic carbonation–decarbonation operating parameters on Zr-doped CaO sorbent CO₂ uptake capacity evolution is examined. It is revealed that the capacity steady state value increases with the decrease in the carbonation temperature, CO₂ concentration in the gas flow upon carbonation and with the increase in the heating rate from the carbonation to the decarbonation stages. The rise in decarbonation temperature leads to a dramatic decrease in the sorbent performance. It is found that if carbonation occurs at 630 °C in the gas flow containing 15 vol.% CO₂ and decarbonation is carried out at 742 °C, the sorbent shows the highest values of the initial and steady state CO₂ uptake capacity, namely, 10.7 mmol/g and 9.4 mmol/g, respectively.

Keywords: CaO-based sorbent; high-energy milling; CO₂ capture; cyclic carbonation–decarbonation; sorbent sintering



Citation: Rodaev, V.V.; Razlivalova, S.S. Performance and Durability of the Zr-Doped CaO Sorbent under Cyclic Carbonation–Decarbonation at Different Operating Parameters. *Energies* **2021**, *14*, 4822. <https://doi.org/10.3390/en14164822>

Academic Editor: Muhammad Akram

Received: 14 June 2021

Accepted: 5 August 2021

Published: 7 August 2021

Publisher's Note: MDPI stays neutral with regard to jurisdictional claims in published maps and institutional affiliations.



Copyright: © 2021 by the authors. Licensee MDPI, Basel, Switzerland. This article is an open access article distributed under the terms and conditions of the Creative Commons Attribution (CC BY) license (<https://creativecommons.org/licenses/by/4.0/>).

1. Introduction

Nowadays, three technologies are considered promising for large-scale post-combustion CO₂ capture, namely, amine scrubbing, pressure swing adsorption and calcium looping (CaL) [1–4]. The main disadvantages of amine scrubbing are a significant energy penalty due to solvent regeneration, equipment corrosion, limitation on the operating temperature, solvent loss and accompanied environment impact. The pressure swing adsorption using physical sorbents is characterized by low selectivity, limitations on operating temperature and high operating pressure to achieve high CO₂ uptake capacity. Both amine scrubbing and pressure swing adsorption can only be used for CO₂ sorption from the flue gas produced during fossil fuel combustion after the flue gas precooling. The use of CaL to capture CO₂ from flue gases was first suggested in 1999 [5]. The CaL process involves the reversible reaction $\text{CaO} + \text{CO}_2 \leftrightarrow \text{CaCO}_3$. CaO is circulated between two fluidized bed reactors called the carbonator and the calciner. The CaL process has a number of major advantages: operating at atmospheric pressure and the use of circulating fluidized bed reactors—a mature technology at a large scale, the energy efficiency penalty is relatively small compared to amine scrubbing, the possibility of selective CO₂ trapping from hot flue gas, synergy with the existing power plants and cement plants and use of sorbent derived from cheap environmentally benign friendly raw materials (limestone and dolomite) [5–7]. The CaL process is also a promising approach for CO₂ utilization since it provides a high-concentrated CO₂ stream during decarbonation [5,6].

CaO is inexpensive and possesses higher CO₂ uptake capacity (the maximum value is about 17.9 mmol/g) compared to alkaline ceramics (for example, Li₄SiO₄—8.3 mmol/g, Li₂ZrO₃—6.5 mmol/g) also suitable for CO₂ capture at elevated temperatures [4].

The main disadvantage of CaO is a rapid decline in reactivity under the cyclic carbonation–decarbonation process caused by the following major factors: low Tammann temperature of CaCO₃, carbonation process high exothermicity and a big difference in molar volumes of CaO (16.9 cm³/mol) and CaCO₃ (36.9 cm³/mol). One of the approaches

used to improve the cyclic stability of CaO is the development of CaO-based synthetic sorbents via incorporation of the dopant into CaO. Inertness to CO₂ in the temperature range of the CaL process and high sintering temperature (Tammann temperature) are the criteria for the dopant selection. The dopant acts as a spacer, preventing CaO/CaCO₃ sintering during cyclic carbonation–decarbonation. The sol–gel method, co-precipitation and flame spray pyrolysis are commonly used to fabricate different CaO-based sorbents [8,9] and, in particular, the Zr-doped CaO sorbents which exhibit superior performance and durability [10,11]. These techniques deal with CaO and the dopant precursors and give rise to nanosized composite sorbents with enhanced CO₂ capture performance and cyclic stability. High-energy milling also ensures efficient particle size reduction and effective dispersion, while being easier to implement, thus this method seems to be more promising for the industrial application than the above laboratory methods [12–14]. Moreover, high-energy milling is the most obvious approach to fabricate composite materials from chemically inert components. In [14] we used high-energy co-milling of calcium carbonate and baddeleyite (natural zirconia mineral), followed by heat-treatment of the obtained nanopowder to fabricate CaO sorbent doped with well-dispersed CaZrO₃ nanoparticles to prevent its sintering. The prepared Zr-doped CaO sorbent was characterized by a high enough steady state CO₂ uptake capacity of 8.6 mmol/g under a multi-cycle carbonation–decarbonation process. The Tammann temperature of CaZrO₃ is 1218 °C [11]. We used natural zirconia since it is much cheaper than chemically synthesized zirconia and its precursors. Previously, high-energy milling has already been successfully applied to baddeleyite to produce engineering-nanostructured zirconia ceramic with competitive mechanical properties [15].

The synthesis method, the nature of the dopant and the dopant concentration in the sorbent are usually considered as the main factors affecting performance and durability of the developed CaO-based sorbents. At the same time, due attention is not paid to the effect of the cyclic carbonation–decarbonation operating parameters on the performance of sorbents, although it is important in terms of prospects and limitations to their practical application.

The aim of this work is to investigate the effect of cyclic carbonation–decarbonation operating parameters on the performance of CaO-based sorbents promoted with chemically inert and heat-resistant dopants on the example of the Zr-doped CaO sorbent produced using high-energy milling. Such operating parameters as carbonation and decarbonation temperatures, CO₂ concentration in the gas flow upon carbonation and the heating rate from the carbonation to the decarbonation stages were varied.

2. Materials and Methods

Baddeleyite concentrate powder (5 µm, 99.3%, Kovdorsky GOK, Kovdor, Russia) and CaCO₃ powder (99.5%, Sigma-Aldrich, Saint Louis, MO, USA) were mechanically mixed to prepare the composite powder with the Zr/Ca molar ratio of 2:10. High-energy milling of the composite powder using distilled water was performed on a planetary mill Pulverisette 7 Premium Line (Fritsch, Idar-Oberstein, Germany) during 5 h. The resulting product was dried in air at 80 °C for 24 h in an OV-11 oven (Jeio Tech Co., Ltd., Seoul, Korea).

The thermal analyzer EXSTAR TG/DTA7200 (SII Nano Technology, Tokyo, Japan) was used to measure CO₂ uptake capacity of the Zr-doped CaO sorbent. Before measurements, the sorbent was activated by heat treatment under N₂ for CaCO₃ decomposition. Then, the sorbent was cooled to the target carbonation temperature at a rate of 10 °C/min and held for 30 min in the gaseous stream of 100 mL/min. The flow of CO₂ and N₂ contained 15, 30, 50 or 100 vol.% CO₂. After carbonation, the sorbent was heated up to the target decarbonation temperature at a rate of 20 °C/min, and held for 20 min under a N₂ flow of 100 mL/min. The carbonation–decarbonation cycle was repeated 25 times. For each cycle, the CO₂ uptake capacity (mmol/g) of the sorbent was determined as the amount of captured CO₂ divided by the sorbent weight before carbonation. The target carbonation and decarbonation temperatures were determined using differential thermogravimetric (DTG) analysis as temperatures when carbonation and decarbonation rates were maximal.

DTG analysis was performed in a N₂ flow when the sorbent was heated from 500 to 900 °C, and in the flow of CO₂ and N₂ with 15, 30, 50 or 100 vol.% CO₂ when the sorbent was cooled from 900 to 500 °C.

The specific surface area (S_{BET}) of the Zr-doped CaO sorbent as microstructure degradation characteristic was measured by nitrogen adsorption at −196 °C in a relative pressure range of 0.05–0.35 with a gas sorption analyzer Autosorb iQ-C (Quantachrome Instruments, Boynton Beach, FL, USA) using the Brunauer–Emmett–Teller (BET) method. All the samples were degassed under vacuum at 300 °C for 3 h before BET analysis.

3. Results and Discussion

According to DTG analysis, the increase in CO₂ concentration in the gas at the sorbent carbonation stage leads to a rise in both carbonation and decarbonation effective temperatures (Figure 1). The positions of the carbonation and decarbonation rate peaks are shifted toward higher temperatures and the peaks become narrower (Table 1).

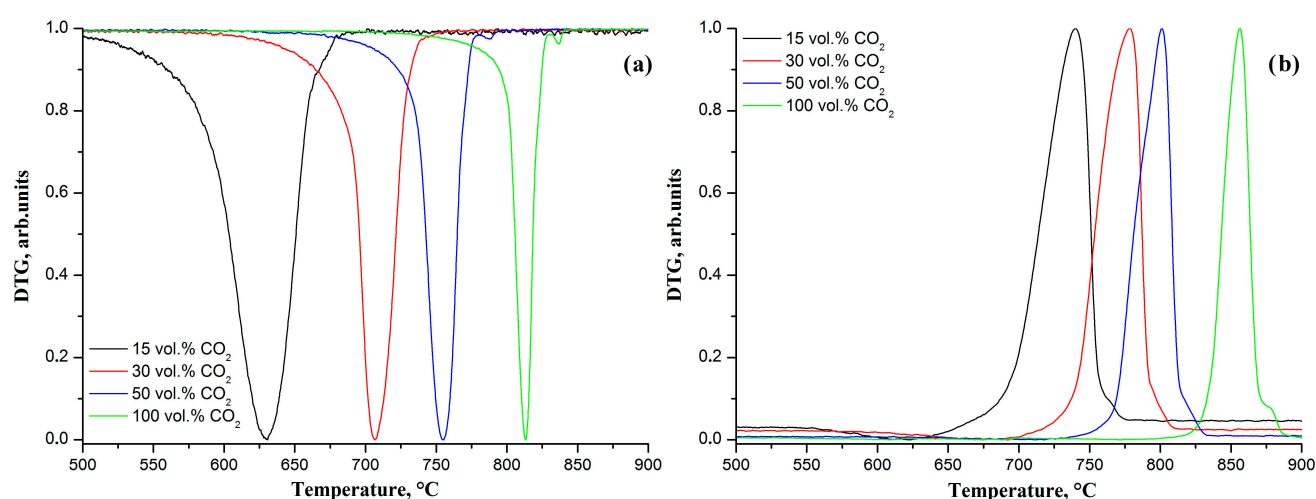


Figure 1. Normalized DTG signals (a) during the sorbent carbonation at different CO₂ concentrations in the gas flow; (b) during the sorbent decarbonation if different CO₂ concentrations are used at the carbonation stage.

Table 1. The carbonation and decarbonation rates peaks characteristics.

CO ₂ Concentrations in the Gas Flow during Carbonation, vol.%	Carbonation Rate Peak		Decarbonation Rate Peak	
	Position T , °C	Peak width at Half Height ΔT , °C	Position T , °C	Peak Width at Half Height ΔT , °C
15	630	48	742	37
30	707	26	779	34
50	755	22	803	27
100	813	14	857	21

The half-height width of the carbonation and decarbonation rate peaks can be considered as the temperature ranges in which the sorbent performs best during carbonation and decarbonation. Table 1 shows that the ranges of operating temperatures of the sorbent depend on CO₂ concentration in the gas flow during carbonation.

The effect of cyclic carbonation–decarbonation on the sorbent CO₂ uptake capacity at different CO₂ concentrations in the gas flow during carbonation is shown in Figure 2. The carbonation and decarbonation are performed at the temperatures indicated in Table 1. It is observed that the initial CO₂ uptake capacity of the sorbent slightly decreases from 10.7 to 10.2 mmol/g with the CO₂ concentration increase from 15 to 100 vol.%. Stoichiometric capacity of the sorbent is about 12.4 mmol/g. The CO₂ uptake capacity of the sorbent decreases with a rise in the cycle number attaining 9.2, 8.9, 8.2 and 7.7 mmol/g in the 25th cycle

at 15, 30, 50 and 100 vol.% CO₂, respectively. The drop in the capacity value increases from 1.5 to 2.5 mmol/g with a rise in CO₂ concentration from 15 to 100 vol.%. The dependence of the sorbent CO₂ uptake capacity on the number of carbonation–decarbonation cycles attains saturation near the 25th cycle if the sorbent is carbonated in the atmosphere containing 15 vol.% CO₂. Thus, it can be concluded that the sorbent is more resistant to cyclic carbonation–decarbonation if carbonation occurs at lower CO₂ concentrations and low temperatures. In further experiments, carbonation is performed at 630 °C in the gas flow containing 15 vol.% CO₂ because such a concentration corresponds to the typical CO₂ content in the exhaust gases of coal-fired power plants and the indicated carbonation temperature corresponds to the average exhaust gases temperature [16].

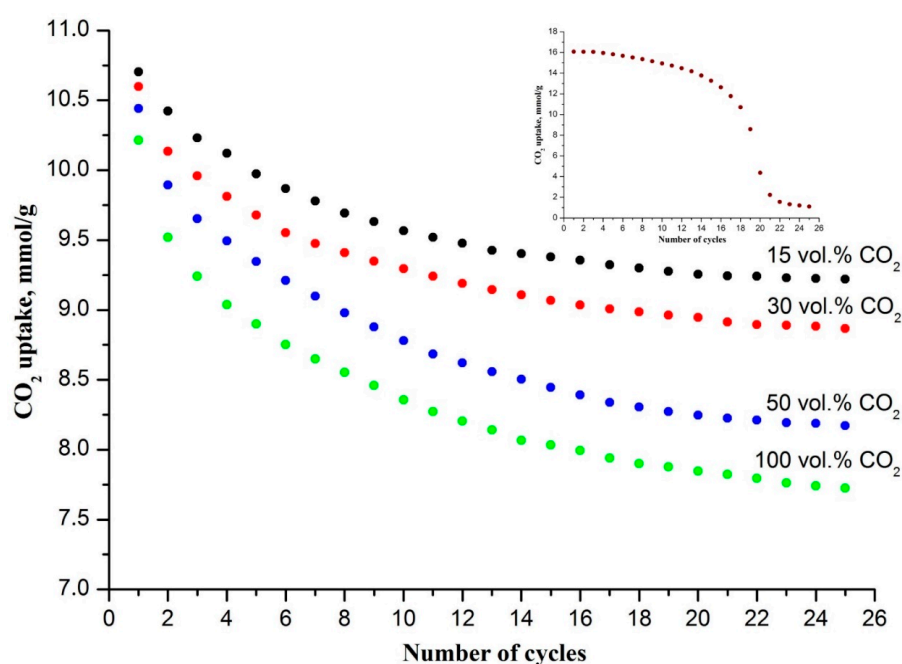


Figure 2. The dependencies of the sorbent CO₂ uptake capacity on the number of carbonation–decarbonation cycles at different CO₂ concentrations in the gas flow upon carbonation. The insert shows the dependence of zirconium-undoped sorbent CO₂ uptake capacity on the number of carbonation–calcination cycles at 15 vol.% CO₂ in the gas flow upon carbonation.

In terms of steady state CO₂ uptake capacity, the studied sorbent is not inferior to CaO sorbents doped with CaZrO₃ previously prepared by co-precipitation (9.6 mmol/g) [17], a sol–gel auto-combustion synthesis (9.2 mmol/g) [18] and the surfactant template/ultrasound-assisted technique (3.4 mmol/g) [19].

It should be noted that if the sorbent is undoped, it shows higher initial CO₂ uptake capacity than the Zr-doped one on a weight basis, due to the inertness of the dopant to CO₂. However, the capacity of pure CaO sorbent decreases dramatically by the 25th cycle (insert in Figure 2).

It has been revealed that both cyclic carbonation–decarbonation and the rise in CO₂ concentration in the gas flow at carbonation lead to a decrease in the sorbent-specific surface area (Table 2). After 25 carbonation–decarbonation cycles, the specific surface area decreases by 3.7, 7.4, 15.2 and 20.3% in relation to the virgin sorbent-specific surface area value of 21.7 m²/g if carbonation occurs in the atmosphere containing 15, 30, 50 or 100 vol.% CO₂, respectively.

Table 2. The sorbent-specific surface area after the 25th carbonation–decarbonation cycle at different CO₂ concentrations in the gas flow during carbonation.

CO ₂ Concentration in the Gas Flow, vol.%	S _{BET} , m ² /g
15	20.9
30	20.1
50	18.4
100	17.3

The Tammann temperature of CaCO₃ is 533 °C [11], which is much lower than the used carbonation temperatures (Table 1). Therefore, CaCO₃ forming during carbonation gets sintered, which has a negative effect on the CO₂ uptake capacity of CaO. Previously, we found that dopant nanoparticles homogeneously dispersed in the tested sorbent separate the sorbent particles from each other, thus hindering CaCO₃ sintering that slows down the CaO particle growth and the sorbent porosity reduction during cyclic carbonation–decarbonation [14]. As a result, the decrease in the CO₂ uptake capacity of the CaO sorbent functionalized by dopant nanoparticles is less pronounced with the increasing number of cycles than the capacity of pure CaO sorbent (Figure 2).

The rise in CO₂ concentration in the gas flow increases the carbonation intensity that results in densification of the CaCO₃ layer forming on the surface of CaO particles, which impedes the penetration of CO₂ deep into the CaO particles; therefore, a higher carbonation temperature is required to provide CO₂ penetration through the product layer, and a higher decarbonation temperature is also required to decompose the dense well-sintered product layer. The CaCO₃ sintering results in CaO particles' growth with each subsequent carbonation–decarbonation cycle. The higher the CO₂ concentration, the more intense the CaO particles' growth at carbonation, which is confirmed by the specific surface area measurements (Table 2).

In [20], it was reported that at the product layer thickness of about 50 nm, an extremely slow diffusion-controlled carbonation stage replaces the fast initial chemical reaction-controlled one. Since the CaCO₃ layer seals CaO inside the sorbent particle and makes it inaccessible for carbonation, the amount of non-reacted CaO increases with each subsequent cycle, due to the sorbent particles' growth. It explains the sorbent CO₂ uptake capacity degradation during cycling (Figure 2). The intensive carbonation induced by a high CO₂ concentration promotes the capacity reduction.

The influence of different decarbonation temperatures on the sorbent CO₂ uptake capacity has been tested too (Figure 3). The carbonation is performed in the gas flow containing 15 vol.% CO₂ at 630 °C (Table 1). The rise in the decarbonation temperature induces a larger drop in CO₂ uptake capacity after the 1st decarbonation. Moreover, at a higher decarbonation temperature the decrease in the CO₂ uptake capacity is more notable with each increasing cycle number. In the 25th cycle, the CO₂ uptake capacity value attains 9.2, 7.6 and 4.5 mmol/g at decarbonation temperatures of 742, 900 and 1000 °C, respectively. The initial CO₂ uptake capacity of the sorbent is 10.7 mmol/g for the given carbonation parameters. The rise in the decarbonation temperature also results in the sorbent-specific surface area decrease (Table 3). After 25 carbonation–decarbonation cycles, the sorbent-specific surface area decreases by 3.7, 21.2 and 53.5% in relation to the virgin sorbent-specific surface area value of 21.7 m²/g. It indicates that the increase in the decarbonation temperature stimulates the CaO particles' growth.

The decarbonation temperature also affects the carbonation kinetics of the sorbent (insert in Figure 3). It is revealed that the time to attain 90% of the maximum capacity value in the cycle increases with the rise in the decarbonation temperature. The chemical reaction-controlled stage becomes shorter and slower, and the diffusion-controlled stage becomes longer and starts earlier.

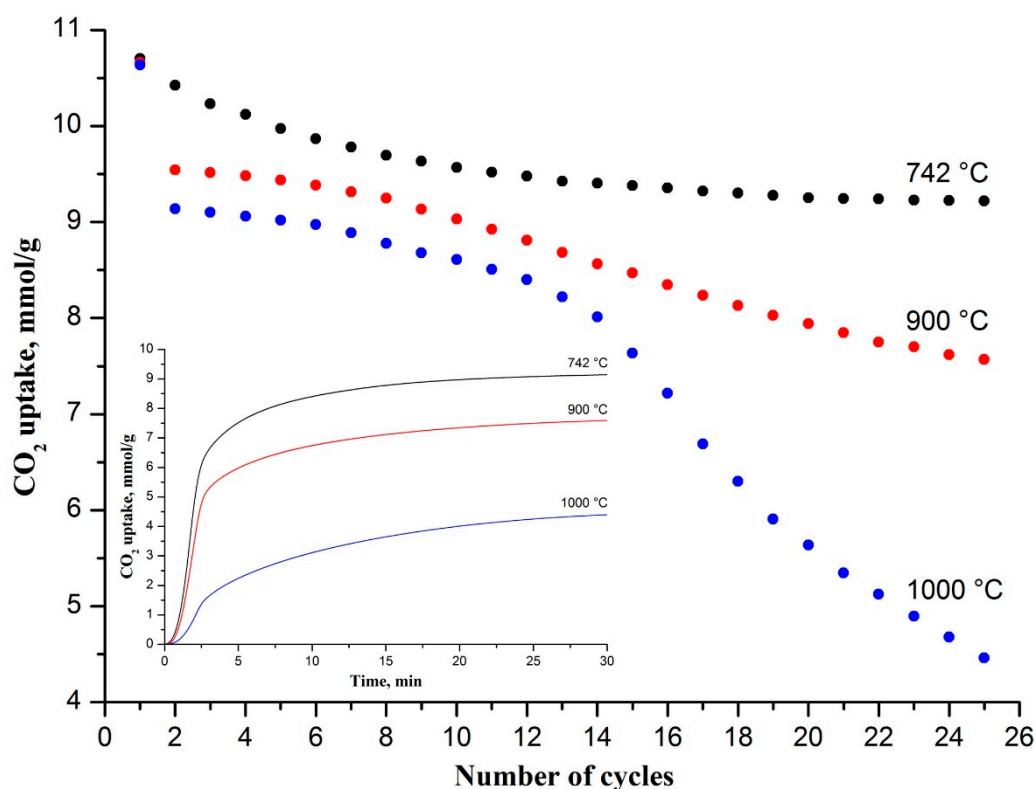


Figure 3. CO₂ uptake capacity evolution of the sorbent over cyclic carbonation–decarbonation at different decarbonation temperatures. The carbonation is performed in the gas flow containing 15 vol.% CO₂ at 630 °C. The insert shows the carbonation profiles of the 25th cycle at different decarbonation temperatures.

Table 3. The sorbent-specific surface area after the 25th carbonation–decarbonation cycle at different decarbonation temperatures.

Decarbonation Temperature, °C	S _{BET} , m ² /g
742	20.9
900	17.1
1000	10.1

CaCO₃ sintering occurs during carbonation, heating up to the decarbonation temperature and upon decarbonation. The Tammann temperature of CaO is 1154 °C [11], which is much higher than the used carbonation temperatures. Therefore, CaO sintering does not occur at carbonation. At a low decarbonation temperature, CaO particle growth is provided only by CaCO₃ sintering. The intensity of CaCO₃ sintering can be reduced, for instance, by increasing the heating rate from the carbonation to the decarbonation stages that decrease CaCO₃ residence time at high temperatures. It is revealed that the sorbent CO₂ uptake capacity decreases less with the rise in the cycle number and reaches a stable value earlier if the heating rate is increased (Figure 4). In the 25th carbonation–decarbonation cycle, the difference in capacity values is 3.6% due to a change in the heating rate from 10 to 40 °C/min.

An increase in the decarbonation temperature leads to CaCO₃ sintering intensification due to heating to a higher temperature. Moreover, when the decarbonation temperature approaches 1154 °C it leads to the start of CaO sintering with partial sintering of CaO particles that additionally promotes CaO particles growth during decarbonation.

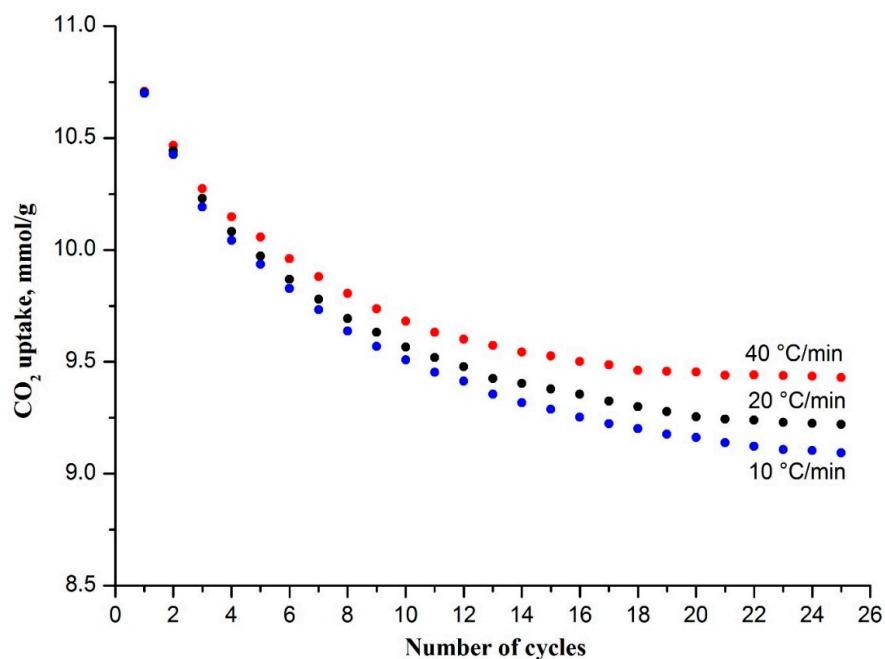


Figure 4. CO₂ uptake capacity evolution of the sorbent over cyclic carbonation–decarbonation at different heating rates. The carbonation is performed in the gas flow containing 15 vol.% CO₂ at 630 °C.

The rise in the CaO particles size decreases the sorbent-specific surface area with the decarbonation temperature increase (Table 3). It indicates that the barrier function of the dopant nanoparticles decreases with an increase in the decarbonation temperature due to diffusion intensification promoting the sorbent sintering. A similar effect was observed in [21], where Nd₂O₃ nanoparticles were used as spacers instead of CaZrO₃ nanoparticles.

CaO sintering hampers CO₂ access to the reaction centers due to gas transport channels blocking. Thus, the amount of trapped unreacting CaO increases with each subsequent decarbonation. It results in the sorbent CO₂ uptake capacity reduction upon cyclic carbonation–decarbonation. Wherein the sorbent CO₂ uptake capacity reduction is greater, the higher the decarbonation temperature (Figure 3). The increased CaO particle size and hindered CO₂ penetration deep into the CaO particles makes a diffusion-controlled mechanism of carbonation dominant when decarbonation occurs at high temperatures (insert in Figure 3).

4. Conclusions

It is revealed that the performance of the Zr-doped CaO sorbent increases with the decrease in the carbonation temperature, CO₂ concentration in the gas flow upon carbonation and with the increase in the heating rate from the carbonation to the decarbonation stages. Contrarily, the performance of the sorbent decreases with the rise in the decarbonation temperature. These operating parameters influence the intensity of sorbent sintering, which in turn affects the sorbent CO₂ uptake capacity during the cyclic carbonation–decarbonation process. It is found that when carbonation occurs at 630 °C in the gas flow containing 15 vol.% CO₂ and decarbonation is carried out at 742 °C, the sorbent shows the highest values of the initial and steady state CO₂ uptake capacity, namely, 10.7 mmol/g and 9.4 mmol/g, respectively. At the decarbonation temperature of 900 °C, which is the typical decarbonation temperature for the CaL process, the capacity steady state value decreases to 7.6 mmol/g.

It can be proposed that variations in the carbonation and decarbonation temperatures, CO₂ concentration in the gas flow upon carbonation and the heating rate from the carbonation to the decarbonation stages might have a similar effect on the performance of all

CaO-based sorbents promoted with chemically inert and heat-resistant dopants, regardless of their fabrication method due to the similar operating principle of such sorbents.

Author Contributions: V.V.R.: investigation, writing—original draft preparation, editing; S.S.R.—investigation. All authors have read and agreed to the published version of the manuscript.

Funding: The reported study was funded by Russian Foundation for Basic Research (RFBR) according to the research project No. 18-29-12015 and partially supported by the Ministry of Science and Higher Education of the Russian Federation in the frame work of agreement No. 075-15-2021-709.

Institutional Review Board Statement: Not applicable.

Informed Consent Statement: Not applicable.

Data Availability Statement: All data included in this study are available upon request from the corresponding author.

Conflicts of Interest: The authors declare no conflict of interest.

References

1. Anwar, M.; Fayyaz, A.; Sohail, N.; Khokhar, M.; Baqar, M.; Khan, W.; Rasool, K.; Rehan, M.; Nizami, A. CO₂ capture and storage: A way forward for sustainable environment. *J. Environ. Manag.* **2018**, *226*, 131–144. [[CrossRef](#)] [[PubMed](#)]
2. Koytsoumpa, E.I.; Bergins, C.; Kakaras, E. The CO₂ economy: Review of CO₂ capture and reuse technologies. *J. Supercrit. Fluids* **2018**, *132*, 3–16. [[CrossRef](#)]
3. Riboldi, L.; Bolland, O. Overview on Pressure Swing Adsorption (PSA) as CO₂ Capture Technology: State-of-the-Art, Limits and Potentials. *Energy Procedia* **2017**, *114*, 2390–2400. [[CrossRef](#)]
4. Bhatta, L.K.G.; Subramanyam, S.; Chengala, M.D.; Olivera, S.; Venkatesh, K. Progress in hydrotalcite like compounds and metal-based oxides for CO₂ capture: A review. *J. Clean. Prod.* **2015**, *103*, 171–196. [[CrossRef](#)]
5. Dean, C.; Blamey, J.; Florin, N.; Al-Jeboori, M.; Fennell, P. The calcium looping cycle for CO₂ capture from power generation, cement manufacture and hydrogen production. *Chem. Eng. Res. Des.* **2011**, *89*, 836–855. [[CrossRef](#)]
6. Tilak, P.; El-Halwagi, M.M. Process integration of Calcium Looping with industrial plants for monetizing CO₂ into value-added products. *Carbon Resour. Convers.* **2018**, *1*, 191–199. [[CrossRef](#)]
7. Coppola, A.; Scala, F. A Preliminary techno-economic analysis on the calcium looping process with simultaneous capture of CO₂ and SO₂ from a coal-based combustion power plant. *Energies* **2020**, *13*, 2176. [[CrossRef](#)]
8. Sun, H.; Wu, C.; Shen, B.; Zhang, X.; Zhang, Y.; Huang, J. Progress in the development and application of CaO-based adsorbents for CO₂ capture—A review. *Mater. Today Sustain.* **2018**, *1–2*, 1–27. [[CrossRef](#)]
9. Hu, Y.; Lu, H.; Liu, W.; Yang, Y.; Li, H. Incorporation of CaO into inert supports for enhanced CO₂ capture: A review. *Chem. Eng. J.* **2020**, *396*, 125253. [[CrossRef](#)]
10. Lu, H.; Khan, A.; Pratsinis, S.E.; Smirniotis, P.G. Flame-made durable doped-CaO nanosorbents for CO₂ capture. *Energy Fuels* **2009**, *23*, 1093–1100. [[CrossRef](#)]
11. Courson, C.; Gallucci, K. CaO-based high-temperature CO₂ sorbents. In *Precombustion Carbon Dioxide Capture Materials*; Wang, Q., Ed.; Royal Society of Chemistry: London, UK, 2018; pp. 144–237.
12. Benitez-Guerrero, M.; Valverde, J.M.; Perejon, A.; Sanchez-Jimenez, P.E.; Perez-Maqueda, L.A. Effect of milling mechanism on the CO₂ capture performance of limestone in the Calcium Looping process. *Chem. Eng. J.* **2018**, *346*, 549–556. [[CrossRef](#)]
13. Sayyah, M.; Lu, Y.; Masel, R.I.; Suslick, K.S. Mechanical activation of CaO-based adsorbents for CO₂ capture. *ChemSusChem* **2013**, *6*, 193–198. [[CrossRef](#)] [[PubMed](#)]
14. Rodaev, V.V.; Razlivalova, S.S. The Zr-Doped CaO CO₂ Sorbent Fabricated by Wet High-Energy Milling. *Energies* **2020**, *13*, 4110. [[CrossRef](#)]
15. Rodaev, V.V.; Zhigachev, A.O.; Korenkov, V.V.; Golovin, Y.I. Spherical engineering Ca-TZP ceramics made from baddeleyite: Fabrication, structure and mechanical properties. *Mater. Sci. Eng. A* **2018**, *730*, 363–366. [[CrossRef](#)]
16. Wang, Y.; Zhao, L.; Otto, A.; Robinius, M.; Stolten, D. A Review of Post-combustion CO₂ Capture Technologies from Coal-fired Power Plants. *Energy Procedia* **2017**, *114*, 650–665. [[CrossRef](#)]
17. Soleimanisalim, A.H.; Sedghkardar, M.H.; Karami, D.; Mahinpey, N. Effects of second metal oxides on zirconia-stabilized Ca-based sorbent for sorption/catalyst integrated gasification. *J. Environ. Chem. Eng.* **2017**, *5*, 1281–1288. [[CrossRef](#)]
18. Antzara, A.; Heracleous, E.; Lemonidou, A.A. Improving the stability of synthetic CaO-based CO₂ sorbents by structural promoters. *Appl. Energy* **2015**, *156*, 331–343. [[CrossRef](#)]
19. Radfarnia, H.R.; Iliuta, M.C. Development of Zirconium-Stabilized Calcium Oxide Absorbent for Cyclic High-Temperature CO₂ Capture. *Ind. Eng. Chem. Res.* **2012**, *51*, 10390–10398. [[CrossRef](#)]

-
20. Alvarez, D.; Abanades, J.C. Determination of the critical product layer thickness in the reaction of CaO with CO₂. *Ind. Eng. Chem. Res.* **2005**, *44*, 5608–5615. [[CrossRef](#)]
 21. Hu, Y.; Liu, W.; Sun, J.; Li, M.; Yang, X.; Zhang, Y.; Xu, M. Incorporation of CaO into novel Nd₂O₃ inert solid support for high temperature CO₂ capture. *Chem. Eng. J.* **2015**, *273*, 333–343. [[CrossRef](#)]